PALACKÝ UNIVERSITY OLOMOUC

FACULTY OF SCIENCE

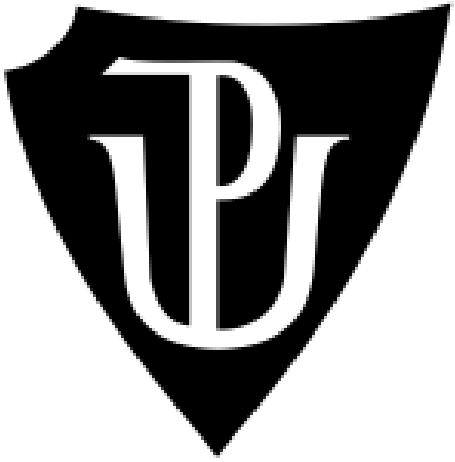

DEPARTMENT OF PHYSICAL CHEMISTRY

Covalently functionalized graphene derivatives for immobilization of Ag nanoparticles as antibacterial nanohybrids

Diploma Thesis

Author: Bc. David Panáček

Subject of study: Materials Chemistry

Form of study: Full-time

Supervisor: Aristeidis Bakandritsos, PhD

Olomouc 2018

Declaration

I declare that I worked independently on my diploma thesis under guidance of Dr. Aristeidis Bakandritsos and all used sources are included in bibliography.

Olomouc …….

…….
Handwritten signature

Acknowledgement

I would like to thank my supervisor Dr. Aristeidis Bakandritsos for valuable advices, opportunities and patience in particular. I would also like to thank doc. RNDr. Aleš Panáček, PhD for many great tips on the preparation of silver nanoparticles. I would also like to thank Dr. Večeřová from the Faculty of Medicine of the Department of Microbiology for performing antibacterial tests, also to thank MSc. Tomáš Steklý for synthesis of graphene derivatives (cyanographene and graphene acid). Last but not least, I would like to thank the Department of Physical Chemistry and Regional Centre of Advanced Technologies and Materials, Palacký University Olomouc for using laboratories and equipment.

Děkuji svým rodičům za podporu, kterou mi poskytli během mého vysokoškolského života a také své přítelkyni za svou trpělivost při mém zkouškovém období.

Bibliografické údaje:

Autor:	Bc. David Panáček
Název práce:	Kovalentně funkcionalizované deriváty grafenu pro imobilizaci Ag nanočástic jako antibakteriálních nanohybridů.
Abstrakt:	V rámci této diplomové práce byly zkoumány kovalentní grafenové deriváty jako substráty pro imobilizaci stříbra. Byly připraveny dva grafenové hybridy: jeden s nanočásticemi stříbra a druhý se stříbrem v iontové formě. Cílem bylo prozkoumat potenciál takových grafen/Ag nanohybridů v antibakteriálních aplikacích. Byl zkoumán antibakteriální účinek hybridů a výsledky ukázaly, že oba materiály vykazují vysokou antibakteriální účinnost proti všem typům testovaných bakterií. Hybridy s iontovým stříbrem měly mírně vyšší aktivitu. Důležité je, že oba tyto materiály byly velmi účinné jak proti bakteriím odolným vůči lékům, tak i bakteriím resistentním proti nanočásticím stříbra.

Typ práce:	Diplomová
Pracoviště:	Katedra fyzikální chemie
Vedoucí práce:	Dr. Aristeidis Bakandritsos
Rok obhajoby:	2018
Klíčová slova:	grafen, stříbro, nanočástice, nanohybrid, antibakteriální aktivita
Počet stran:	46
Jazyk:	Anglický

Bibliographical identification:

Author:	Bc. David Panáček
Title:	Covalently functionalized graphene derivatives for immobilization of Ag nanoparticles as antibacterial nanohybrids.

Abstract: In the frame of this diploma thesis covalent graphene derivatives were studied as substrates for the immobilization of silver. Two types of graphene hybrids were prepared: one with silver nanoparticles and a second with silver in ionic form. The aim was to explore the potential of such graphene/Ag nanohybrids in antibacterial applications. Antibacterial activity of the hybrids was investigated and results showed that both materials exhibit high antibacterial activity against all types of bacteria tested. The hybrids with ionic silver and ultra-small Ag nanoparticles had slightly higher activity. Importantly, both of these materials were very effective even against drug-resistant and silver resistant bacteria.

Type of work:	Thesis
Supervisor:	Dr. Aristeidis Bakandritsos
The year of presentation:	2018
Department:	Department of Physical Chemistry
Keywords:	graphene, silver, nanoparticles, nanohybrid, antibacterial activity
Number of Pages:	46
Language:	English

Table of contents

1. Introduction

Complications related to infectious diseases have significantly decreased due to the availability and use of a wide variety of antibiotics and antimicrobial agents. However, excessive use of antibiotics and antimicrobial agents over years has increased the number of drug resistant pathogens. Microbial multidrug resistance poses serious risks and consequently research attention has refocused on finding alternatives for antimicrobial treatment. Among the various approaches, the use of engineered nanostructures is currently the most promising strategy to overcome microbial drug resistance by improving the remedial efficiency due to their high surface-to-volume ratio and their intrinsic or chemically incorporated antibacterial activity. Graphene, a two-dimensional ultra-thin nanomaterial, possesses excellent biocompatibility, putting it in the forefront for different applications in biosensing, drug delivery, biomedical device development, diagnostics and therapeutics. Graphene-based nanostructures also hold great promise for combating microbial infections.[1]

Infectious diseases caused by pathogenic microorganisms such as viruses, bacteria and fungi are still one of the world's most challenging global health issues. While morbidity and mortality from infections decreased considerably from the late 1940s onwards due to the commercialization and use of penicillin, issues related to the emergence of many microorganisms that have become resistant to antibiotics have made the search for the treatment of infectious diseases again of high importance. For example, some of the Gram-positive (e.g. Staphylococcus aureus) and Gram-negative (Escherichia coli, Pseudomonas aeruginosa) bacteria are the common multi-drug resistant (MDR) pathogens and important causes of various often hospital-acquired infections. According to published data in 2011, 25 000 patients die annually in the EU as a result of infections caused by antibiotic resistant bacteria, with two-thirds of these deaths due to Gram-negative pathogens. The report entitled ''Review on Antimicrobial Resistance'' published in December 2014 by J. O-Neill estimates a death quote attributable to antimicrobial resistance (AMR) of 10 million in 2050. The costs incurred by drug resistant infections amount to an estimated 1.5 billion annually, due to the increase in healthcare expenditure costs.[2]

2. General Background

2.1 Colloidal systems

Colloidal systems are one of the three main possible states of the so-called dispersion systems, which are composed of two parts: dispersed phase and dispersion environment (solid, liquid or gas). The dispersion environment (solvent in the case of liquid) forms a continuous phase in the system, in which the dispersed phase is embedded. If the dispersion system contains two components but only one phase (macroscopically), this system is homogeneous. Conversely, if the dispersion system contains two phases, one solvent-rich and the other rich in dispersed phase, this system is termed heterogeneous. Colloidal dispersions are considered the homogeneous systems where the size and density of the dispersed phase is such that its motion is dominated by the Brownian phenomena and not from the gravity: there the dispersed phase does not separate by precipitation. In general, the particle size in a colloidal system lies in the range of 10^{-9} - 10^{-6} m. Colloids typically scatter visible light considerably, also known as Tyndall effect,[3] (since light scattering is maximized when it's wavelength is of same order of magnitude as that of the particle), unlike the case of the typical molecular solutions.[3]

2.1.1 Division of colloidal systems

Due to diversity, we can divide colloidal systems into multiple classes according to many criteria. For example, depending on the shape or size of the dispersed particles or on the state of the dispersion environment and dispersion phases. If all particles of the disperse phase are of the same size, such a system is monodisperse. If the particles have different sizes the system is termed polydisperse.

The particles or the system can be divided into laminar, corpuscular and fibrillar dispersions. Laminar particles are plate-shaped (only one dimension restricted at the micro- or nanoscale). Corpuscular particles are spherical particles with all three dimensions at the micro- or nanoscale. Fibrillar particles take the form of either rods or filaments (two dimensions at the micro- or nanoscale).[3]

2.2 Optical properties of colloidal systems

Describing the optical properties of colloidal systems is a complicated matter. Once the light beam (electromagnetic radiation) strikes the colloidal system, both radiation absorption and scattering of incident radiation occur. Depending on the nature of the colloid system (chemical composition of the disperse phase, particle size), one of the phenomena prevails.[3]

2.2.1 Light scattering

A light scattering occurs when the light beam passes through the colloidal dispersion. All such systems exhibit the so-called Tyndall effect (scattering light beam into the cone).

To illustrate dispersion of light in dispersion systems, Mie's vector diagrams are used. The diagram shows quantities such as the intensity of polarized and non-polarized light in the form of radius vectors to all sides from the particle display point. For the description of light scattering, Rayleigh had developed a theory that was applicable only to small particles that must be spaced apart and show no radiation absorption.[4]

According to this theory, the relationship of the intensity of the scattered radiation of the vertically polarized light component was derived.

$$\left(\frac{I}{I_0}\right)_V = \frac{16\pi^4 R^6}{r^2\lambda^4} \cdot \left(\frac{n_{rel}^2 - 1}{n_{rel}^2 + 2}\right)^2$$

Equation 1: The relationship of the intensity of the scattered radiation of the vertically polarized light component.

$$\left(\frac{I}{I_0}\right)_V = \frac{16\pi^4 R^6}{r^2\lambda^4} \cdot \left(\frac{n_{rel}^2 - 1}{n_{rel}^2 + 2}\right)^2 (\cos^2\theta)$$

Equation 2: Horizontal component of polarized light, which is dependent on the direction of observation.

where R is the radius of the particle, r the distance of the detector, λ is the wavelength of the original and dispersed radiation in the dispersed medium, and nrel is the relative refractive index.

2.2.2 Dynamic light scattering

Dynamic Light Scattering (DLS) is a method suitable for particle size measurement in the submicron range. The basis of this technique is to measure the fluctuation of light diffusion intensity from the laser source around its average value. These fluctuations are related with interference's weakening and amplification of light scattered on non-stationary particles of the disperse phase subject to Brown's motion. The faster the particles move, the faster the intensity of the diffused light changes. The rate of these changes is therefore directly dependent on the movement of the molecule.[5] The particle size measured by dynamic light scattering is based on the diameter of the sphere, which diffuses at the same rate as the measured particle. The size is determined first by measuring Brown's particle motion in the sample using dynamic light scattering and then calculating the particle size based on Einstein's equation. Small particles are known to move rapidly in the fluid and the large ones slowly. This movement is continuous, so when we take into account two systems with different particle sizes, we observe the time scales of their movement, more precisely how many the particles have moved. Thus, it is possible to calculate how large the particle is. If the minimum movement and position of the particles are very similar, the particles in the sample will be large; Similarly, if there is a large movement and the position of the particles is completely different, then the particles in the sample are small.[6]

2.2.3 Absorption of light

When absorbing light, the amount of energy of electromagnetic radiation is absorbed by matter. This leads to a change in the energy states of the valence and bonding electrons. When absorbing radiation, the internal energy of the system's molecules, which changes in thermal energy, increases.

A story where a substance absorbs light is captured by Lambert-Beer's law[7]

$$\mathbf{A= -log\frac{I}{I_0} = \varepsilon cd}$$

Equation 3. Lambert-Beer's Law

where I is the intensity of light passing through the substance, I0 is the intensity of incident light on the substance, ε is the absorption coefficient, c is the absorption concentration, d is the thickness of the layer, and A is the absorbance quantity.

Metal nanoparticles absorb specifically light of a particular wavelength associated with electron oscillations in the conduction band of very small particles - we call this phenomenon as surface plasmon.[8]

2.3 Electrical properties of colloidal systems

In many colloid systems with an aqueous medium, the phase interface carries an electrical charge whose importance is mainly in the stability of these systems.[9]

2.3.1 Electric double layer

If the charged surface of the particle is in contact with the solution ions, the opposite sign ions are attracted. The charge of these ions neutralizes the charge of the surface, and a kind of formation is formed which is made up of two layers. These layers are oppositely charged and form the so-called electric double layer. There is a difference in electrical potential between the charged surface and the bulk phase of the solution. The inner part of the double layer is designated as an inner layer or a charged surface. This layer is either a part of a solid phase or forms on the surface an adsorbed layer of one ionic thickness. It can be considered an area that carries an electric charge Q0. The charge per unit surface area is called the area charge density: $\sigma 0 = Q0 / A$. The inner layer attracting the opposite ions of the solution forms a second layer of the same density of the charge but with the opposite sign - the outer layer. The outer layer is bound to the inner layer by both electrical and adsorption forces.[10]

2.3.2 Electrokinetic potential

Most liquids contain some ions, which are either negatively charged or positively charged, anions, cations. When a charged particle is contained in a liquid, ions with an opposite charge other than the charge of the particle in the liquid are attracted to the surface of the suspended particle. The negative charge particles will attract positively charged ions from the liquid and vice versa. The ions, which are closer to the surface of the particle, they are bonded strongly. While the ions that are farther away will bind more freely and will form the so-called diffusion layer. Within the diffusion layer there is an imaginary boundary where the ions are moving with particles in the liquid. On the other hand, there are some ions outside this boundary that do not move and remain in the original place - this is called the Slipping plane or the motion interface. There is a potential that varies between the surface of the particle between the particle surface and the liquid. This potential is Zeta-potential ζ.[6]

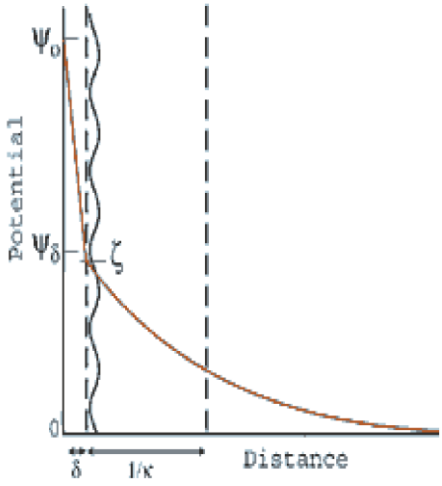

Figure1. Scheme of electric double layer and distribution of electrical potential.[11]

2.3.3 Stabilization of colloidal systems

The stability of dispersing systems ranges over a wide range, from total instability to almost complete stability. The thermodynamic stability and kinetic stability are assessed in the stability of the dispersion systems. Kinetic stability is a process in which the system preserves the distribution of particle concentration in the gravitational field. Aggregate stability is then related to thermodynamic stability - it is some stability when the system maintains a given degree of dispersion. Systems that contain large particles appear to be kinetic instabilities. The smaller the particle size, the more aggregate instability applies.[12]

2.3.4 Steric stabilization

Substances that are soluble in the dispersion medium and also capable of sufficiently large adsorption to the surface of the lyophobic particles are mediated by steric stabilization. As a result, lyophobic particles are more stable, free of coagulation and lyophilized surface. For steric stabilization, surfactants are used which form associative colloids and some macromolecules.[12]

2.3.5 Stabilization by electric double layer

The principle of this stabilization is in an electric double layer formed around particles that have electrically charged surface and are able to attract the opposite charge ions. As the particle moves, the portion of the charge with the opposite sign in the outer diffusion layer binds so that the particle appears to be electrically charged. All particles belonging to the same substance in the same dispersion environment have the same charge and therefore, in the event of a collision, the electrostatic force is removed against the adhesive forces. This leads to the particles being separated from each other again and the connection does not occur.[12]

2.4 Preparation of colloidal systems

There are two quite different ways to prepare colloidal systems - on one hand, there are dispersing methods where macroscopic substances break down into particles of colloidal proportions, and on the other are condensation methods that produce molecular aggregates of colloidal size.[13] They are also usually termed top-down and bottom-up, respectively.

2.4.1 Condensation methods

These methods are divided into two groups, namely physical and chemical. In physically condensing processes, the solubility of substances in which the change of solvent results in condensation of the substance to form colloidal particles is taken into account.

The preparation of silver nanoparticles through chemical methods is the most common today. Chemical methods are based on the reduction of silver salt. Reduction are used as inorganic agent such as sodium borohydride, hydrazine or hydrogen peroxide and the organic reducing agents, among them sodium citrate, ascorbic acid or a reducing sugar.

Due to the strong reducing agent, such as sodium borohydride, small monodisperse particles are formed. Citrate as a representative of a weaker reducing agent causes the formation of larger polydisperse particles.[14]

Nowadays, controlled synthesis using the Tollen's method, which is based on the reduction of silver ammoniacal glucose solution, is increasingly used.[15]

2.4.2 Dispersing methods

Colloidal systems can be obtained after reduction of the size of the dispersed phase by, for example, laser ablation, milling or electrical spraying. Practical application has arc distraction and laser ablation. [16]

2.5 Graphene

Graphene is an atomically thin sheet composed from carbon atoms, which is the basic structural unit of graphite, representing only one layer. At first, this two-dimensional material was studied only theoretically, but it was consider thermodynamically unstable. In 2004, scientists Geim and Novoselov separated one layer of graphite by mechanical way called exfoliation.[17] This layer was subsequently studied several techniques. Exciting properties where discovered such as an extreme surface area, high electron mobility, or optical absorption of 2.3%, stimulating the interest in 2D materials worldwide.

2.5.1 Structural properties

Carbon atoms in the graphene sheet create a planar structure with every atom in sp^2 hybridization with bond length of 1.425 Å. One 2s and two 2p orbitals are hybridized and the $2p_z$ orbital is none hybridized. This orbital is occupied by one electron, which allows it to interact with other non hybridized $2p_z$ orbitals from the neighboring carbons. Due to planarity of the structure, there is conjugation of 6 π electrons in every hexagonal ring and therefore graphene is an aromatic structure according to Hückel's aromaticity rule. Graphene is many times stronger than steel (of similar dimensionality), being furthermore flexible and chemically stable.[18]

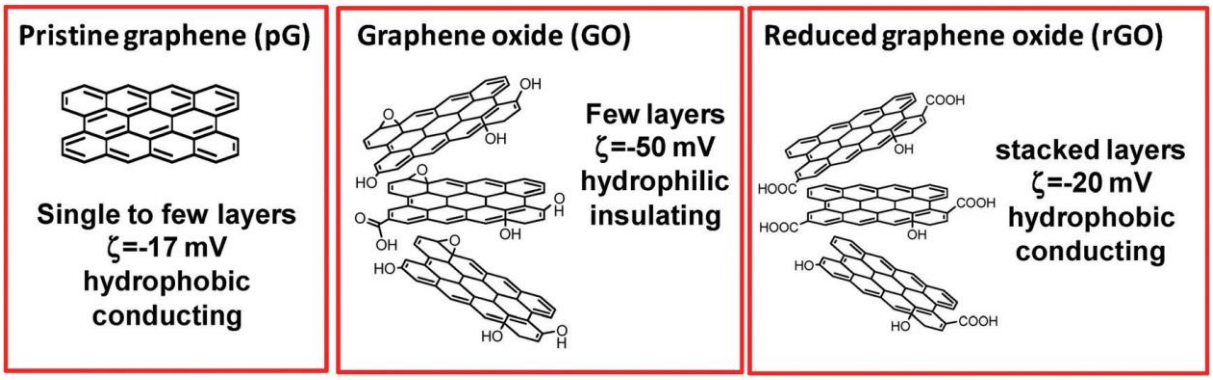

Figure 2. Graphene family. Images reproduced from reference [1]

2.5.2 Synthesis of Graphene and Graphene oxide

Single-layer transferable graphene nanosheets were first obtained by mechanical exfoliation ("Scotch-tape" method) of bulk graphite and by epitaxial chemical vapor deposition.[17,19] Although those routes might be preferred for precise device assembly, they can be less effective for large-scale manufacturing. Chemical means are a practical approach for large-scale production of graphene materials.[20] The primary obstacle towards single or few-layer graphene is the enormous interlayer van der Waals forces. To date, chemical efforts at graphite exfoliation have been focused primarily on intercalation, chemical derivatization, thermal expansion, oxidation/reduction, the use of surfactants, or some combination thereof.[21] The most common approach to graphite exfoliation is the use of strong oxidizing agents to yield graphene oxide (GO), a nonconductive hydrophilic carbon material.[22] Although the exact structure of GO is difficult to determine, it is clear that for GO the previously contiguous aromatic lattice of graphene is interrupted by epoxides, hydroxyls, ketones carbonyls, and carboxylic groups.[23] The disruption of the lattice is reflected in an increase in interlayer spacing from 0.335 nm for graphite to more than 0.625 nm for GO.[24] Brodie first demonstrated the synthesis of GO in 1859 by adding a portion of potassium chlorate to a slurry of graphite in fuming nitric acid.[25] In 1898, Staudenmaier improved on this protocol by using concentrated sulfuric acid as well as fuming nitric acid and adding the chlorate in multiple aliquots over the course of the reaction. This small change in the procedure made the production of highly oxidized GO in a single reaction vessel significantly more practical. In 1958, Hummers reported the method most commonly used today: the graphite is oxidized by treatment with $KMnO_4$ and $NaNO_3$ in concentrated H_2SO_4.[26] The most common source of graphite used for chemical reactions, including its oxidation, is flake graphite, which is a naturally occurring mineral that is purified to

remove heteroatomic contamination.[27] GO prepared from flake graphite can be readily dispersed in water and has been used on a large scale for preparing large graphitic films, as a binder for carbon products, and as a component of the cathode of lithium batteries. Moreover, the hydrophilicity of GO allows it to be uniformly deposited onto substrates in the form of thin films, which is necessary for applications in electronics.[28] It is also often essential that the GO can be transformed back into a conductive graphitic material, and indeed, either in thin films or in bulk, partial restoration of the graphitic structure can be accomplished by chemical reduction to chemically converted graphene (CCG).[29] However, the graphitic structure (with its desired properties) is not fully restored using these conditions, and significant defects are introduced.[30] Currently, Hummers' method ($KMnO_4$, $NaNO_3$, H_2SO_4) is the most common method used for preparing graphene oxide. It was found that excluding the $NaNO_3$, increasing the amount of $KMnO_4$, and performing the reaction in a 9:1 mixture of H_2SO_4/H_3PO_4 improves the efficiency of the oxidation process. This improved method provides a greater amount of hydrophilic oxidized graphene material as compared to Hummers' method or Hummers' method with additional $KMnO_4$. Moreover, even though the GO produced by this method is more oxidized than that prepared by Hummers' method, when both are reduced in the same chamber with hydrazine, chemically converted graphene (CCG) produced from this new method is equivalent in its electrical conductivity. In contrast to Hummers' method, the new method does not generate toxic gas and the temperature is easily controlled. This improved synthesis of GO may be important for large-scale production of GO as well as the construction of devices composed of the subsequent CCG.[31]

2.5.3 Carboxylated graphene (Graphene acid)

Graphene acid can be considered as an alternative material to GO, but unlike Go it is functionalized selectively with carboxyl groups. The rest of the carbon atoms are in sp2 hybridization, thus imparting substantial conductivity (unlike GO). Graphene acid is produced by acidic hydrolysis of cyanographene. The latter is synthesized via the controllable defluorination of fluorographene and substitution of F atoms with nitrile groups. The highly conductive and hydrophilic cyanographene allows exploiting the chemistry of −CN groups toward a broad scale of graphene derivatives with very high functionalization degree. Graphene acid, a 2D carboxylic acid with pKa of 5.2, shows excellent biocompatibility, conductivity and dispersibility in water. Furthermore, the carboxyl groups enable simple, tailored and widely accessible 2D chemistry onto graphene.[32]

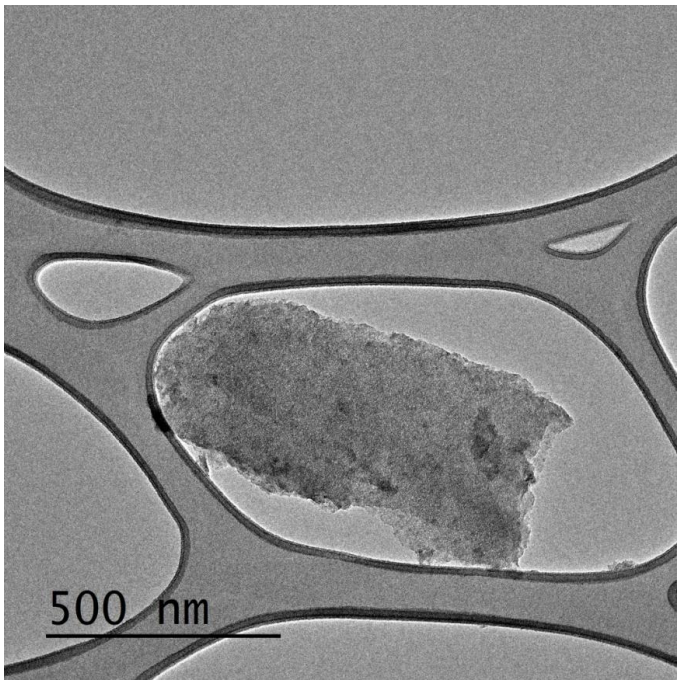

Figure 3. HR-TEM image of a few-layered G-COOH flake.

2.5.4 Antibacterial activity

Recently, graphene has been proposed as a novel effective antibacterial material, with a severe cytotoxici effect on bacteria fungi and plant pathogens with little resistance.[33] Moreover, in comparison with carbon nanotubes, graphene displays tolerable effect on mammalian cells. In addition, graphene is renewable, easier to obtain, and cheaper than metals and metal oxides.[34]

In general, the antibacterial action of graphene involves both physical and chemical effects. Physical damages are induced mainly by the direct contact of its sharp edges with bacterial membranes and destructive extraction the lipid molecules. The wrapping and photothermal ablation mechanisms are also involved. The chemical effect is primarily oxidative stress created by reactive oxygen species (ROS) or charge transfer. Furthermore, Graphene has been used as a support to

disperse and stabilize various nanomaterials, such as metals, metal oxides, polymers, and their composites, with high antibacterial efficiency due to the synergistic effect.

Physical damage of bacterial membranes by sharp edges is the most important mechanism of the antibacterial activity of graphene. Graphene oxide (GO) and reduced graphene oxide (rGO) are efficient inhibiting the growth of Escherichia coli.[35] By surveying the efflux of the bacteria cytoplasmic materials, it was concluded that direct contact of the sharp edges of graphene nanowalls with bacterial membranes led to bacterial inactivation.[36] The cell membrane was disrupted by the graphene nanosheets, and the incomplete membrane subsequently mediated the release of functional enzymes such as β-D-galactosidase and electrolytes from the bacterial cell, ultimately leading to death.[37]For the antibacterial activity of graphene nanosheets, the density of their edges was considered to be one of the key factors. The sharp edge could cut through the bacterial cell membrane to form pores, which subsequently led to osmotic imbalance and bacterial death.[38]

2.6 Silver Nanoparticles

Silver in various forms like metallic silver or silver salts has been used as an effective antibacterial agent for many centuries and has retained effective antibacterial activity throughout that period. From the beginning of the 20th century, colloidal silver replaced most of toxic silver salts and become common therapeutic agent for treatment of systemic and local infections. A typical example is a silver sulfadiazine, which remains popular as a local bacteriostatic in a treatment of burns and mould infection.[39]

Recently, attention has been paid to research into the antibacterial activity of colloidal dispersion of silver nanoparticles. Nowadays, silver nanoparticles and nanocomposites are among the most attractive nanomaterials and have been widely used in a range of biomedical applications including diagnosis, cancer treatment, drug delivery and antibacterial coatings for surgical instruments, catheters, contact lenses, breathing masks, tracheal tubes or bandages because of their high antimicrobial efficiency.[40]

2.6.1 Preparation of silver nanoparticles

Nowadays, great deals of silver nanoparticles are being explored, but among those usable in terms of particle stabilization and their size distribution are just a few of suitable.

The most commonly used preparation of silver nanoparticles is the chemical reduction of a silver salt solution by a reducing agent such as sodium borohydride and ascorbic acid.[41,42] Using of a strong reducing agent such as NaBH4, makes small particles with almost monodisperse system. The synthesis of Ag colloid particles was tried to prepare by using a two-step reduction process, to control the particle size. In this procedure, a strong reducing agent was first applied to form small silver particles, which were magnified in a secondary step by a weaker reducing agent.[42] This method is very difficult to control the poly polydispersibility of the system. The use of these reducing agents may be closely related with environmental toxicity or biological hazards and this has led to development eco friendly synthesis of silver colloid nanoparticles. Tollen's method of preparation was designed to solve this problem with toxicity and in order to demonstrate the creation of controlled-sized silver particles in a one-stage process.[43] The basis of this reaction is the reduction of a silver ammoniacal solution using saccharides as reducing agents. In this Tollen's procedure, films with colloidal silver particles ranging from 50 to 200 nm. This more recent study uses the difference in the redox potential of reducing agents and silver ions for controlled particle formation that have been reduced.[14] This difference was easily controllable by changing the concentration of complexing agent, ammonia, of the silver ion, and using a range of reducing saccharides (glucose, fructose, and maltose). This way formed silver colloid particles with sizes ranging from 45 to 380 nm. This preparation of silver nanoparticles is an environmentally friendly because of the use of nontoxic chemicals. Thanks to this preparation, particles can be obtained with size approximately 25-50 nm and with very low polydispersity index. All preparation methods have a major problem with particle stabilization and subsequent durability. This problem can be solved by introducing gelatin into the solution in a given preparation, where gelatin serves as an excellent particle stabilizer against subsequent aggregation.[43]

2.6.2 Antibacterial Activity

Silver (Ag) has been used in antibacterial agents for centuries. The released Ag ions can destroy bacterial cell membranes and penetrate the cells to inactivate enzymes and cause cell death. Silver nanoparticles (AgNPs) can cause direct damage to the bacterial cell membrane. Bacteria may be killed by the combined bactericidal effects of the released Ag ions and AgNPs.

Silver nanoparticles exhibit high bactericidal activity at concentrations that are not cytotoxic to human cells and also strongly enhance the antibacterial activity of conventional antibiotics even against multiresistant bacteria through synergistic effects. However, bacteria have developed resistance to ionic silver as well as silver nanoparticles.[44]

Mechanism of resistance to ionic silver involves active efflux of Ag+ from the cell by P-type adenosine triphosphatases or chemiosmotic Ag+/H+ antiporters. Mechanism of resistance to silver nanoparticles is very specific and different. This resistance is due to the production of flagellin, an adhesive protein of the bacterial flagellum, which causes the aggregation of silver nanoparticles and thereby eliminates their antibacterial effect against Gram-negative bacteria. Importantly, the developed bacterial resistance can be suppressed by treatment with inhibitors of flagellin production such as pomegranate rind extract. These findings clarify a mechanism that can drive bacterial resistance to antibacterial agents and will be useful in preventing bacterial drug resistance and the fight against infectious bacteria. Another option is a prevention of the aggregation of silver nanoparticles by solid immobilization to a suitable substrate.[45]

2.7 Graphene/Ag composite

AgNPs aggregate when they come in contact with bacteria; thus, they lose their active surface area and show weaker antibacterial activity. To overcome this problem, nanocomposites composed of graphene and AgNPs are being studied.[46]

Graphene oxide/silver nanoparticles (GO-Ag) composites were prepared and their antibacterial properties against Xoo (Xanthomonas oryzae-plant disease) were investigated. The results showed that the GO-Ag composite displayed a fourfold improvement as compared to that of pure Ag NPs.[47] In another work, a new type of chemically modified graphene oxide (GO) was synthesized where a silane ligand was used for stabilizing monodispersed and small Ag nanoparticles. The

antibacterial activity of this hybrid against E. coli and S. aureus was determined to be 0.6 and 1.2 mg/ml of silane ligand-modified graphene oxide (LG-Ag). Antibacterial activity against S. aureus is lower than that against E. coli, probably due to the difference in cell walls.[48] Graphene quantum dot hybrids with Ag nanoparticles (GQD/AgNP hybrids) were proposed as oxidase mimics and antibacterial agents. In accordance with their prominent enzyme activities, the GQD/AgNP hybrids show excellent antibacterial properties against Gram-negative and Gram-positive bacteria, as well as drug resistant bacteria (Escherichia coli and Staphylococcus aureus[49]). The composite based on metal-graphene oxide (MGO-Ag) was synthesized by doping silver and Fe_3O_4 nanoparticles on the surface of GO for the purpose of efficient and safe disinfection.[50] Pant et al. reported that aminophenol functionalized silver particles anchored on the graphene surface displayed 100% antibacterial activity after its incubation for 8h, but it could not be separated efficiently for recycling the material. Tian's et al. developed GO- Ag NP nanocomposite as a novel multifunctional antibacterial material and displayed 93.9%, 85.3% inactivation to E. coli and S. aureus, respectively, at the concentration of 8 μg/mL. In comparison, MGO-Ag exhibited superior antibacterial efficiency, at concentration as low as 6.25 μg/mL. After the antibacterial tests, the material could be easily separated by an external magnet.[50] Pure GO dispersion does not display any obvious inhibition of the bacterial growth even at the highest concentration tested. This result is in good agreement with other reported observations which point out the weak and often controversial antimicrobial effect of GO. Probably the degree of oxidation and the size of the GO flakes play a decisive role onto their antibacterial activities. On the contrary, AgNPs–GO nanohybrids exhibit a significant antibacterial activity and inhibit the bacterial growth in a concentration dependent manner after 24 hr of incubation. The minimal concentration to inhibit bacterial growth (MIC) value obtained for AgNPs–GO nanohybrids is lower than those observed previously. However, a smaller MIC value was demonstrated in the case of chitosan-coated AgNPs as a result of synergistic activity of chitosan and AgNPs. Chit–AgNPs–GO nanohybrids exhibited increased bacteriostatic effect as compared with AgNPs–GO nanohybrids against two strains of MRSA.[51]

The emergence of antibiotic-resistant bacteria is a major threat to world-wide public health. Functionalized nanoparticles could offer novel strategies in this post-antibiotic era. Nanocomposites of silver nanoparticles decorated with graphene quantum dots (Ag-GQDs) have been developed using pulsed laser synthesis. Concentration of 25 and 50 *u*g/mL are required for Ag-GQDs to inhibit the growth of S. aureus and P. aeruginosa bacteria.[52] Graphene oxide (GO) decorated with biogenic silver nanoparticles (Bio-AgNPs) produced by the fungus Fusarium oxysporum displayed

a potent biocidal activity against the Salmonella typhimurium strain at a concentration of 2.0 ug/mL.[53] Graphene oxide (GO) sheets decorated with amino acid L-cysteine (L-cys) functionalized silver nanoparticles (GO-L-cys-Ag) was synthesized by reduction of $AgNO_3$ with $NaBH_4$. Antibacterial activity tests of GO-L-cys-Ag nanocomposite were carried out using Escherichia coli and Staphylococcus aureus as model strains of Gram-negative and Gram-positive bacteria, respectively. Morphological observation of bacterial cells by scanning electron microscope showed that GO-L-cys-Ag nanocomposite was more destructive to cell membrane of Escherichia coli than that of Staphylococcus aureus. The bactericidal property of GO-L-cys-Ag nanocomposite could have a wide range of application in the field of biomedical science.[54]

3. Experimental part

3.1 Materials and reagents

The following chemical were used: Silver nitrate (p.a., Fagron), ammonia (28–30% [w/w], p.a., Sigma-Aldrich), sodium hydroxide (p.a., Lach-Ner), graphene acid, cyanographene, sodium borohydride (Sigma-Aldrich), sodium citrate dehydrate (p.a., Sigma-Aldrich). All solutions were prepared with demineralized water (produced by MERCI AQUAL29) with a conductivity of 0.05 μS / cm. The covalent graphene derivatives (cyanographene and graphene acid) were prepared according to previous procedures.[55] The concentrations of the reaction components were as follows: Cyanographene 750 mg/L; Graphene acid 750 mg/L; silver nitrate 2.2×10^{-3} mol/L; ammonia 3.2×10^{-3} mol/L; sodium borohydride 2.2×10^{-3} mol/L; sodium citrate dihydrate 6.9×10^{-3} mol/L.

The following standard reference strains (labelling according to Czech Collection of Microorganism, Masaryk University, Brno, Czech Republic) were used for antimicrobial activity determination: *Staphylococcus aureus* CCM 3953, *Enterococcus faecalis* CCM 4224, *Escherichia coli* CCM 3954, and *Pseudomonas aeruginosa* CCM 3955. Further, the following bacterial strains isolated from human clinical material at the University Hospital, Olomouc, Czech Republic, were used on testing of antimicrobial activity: *Staphylococcus aureus* 008, multi-resistant *Escherichia coli* 5556, *Pseudomonas aeruginosa*, methicillin-susceptible *Staphylococcus epidermidis*, methicillin-resistant *Staphylococcus epidermidis*, methicillin-resistant *Staphylococcus aureus* (MRSA), vancomycin-resistant *Enterococcus faecium* (VRE), and ESBL-positive *Klebsiella pneumoniae.* Antimycotic activity was tested using *Candida albicans* strain isolated from the blood of those patients at the University Hospital Olomouc who had confirmed *Candida sepsis*. Strains of bacteria resistant to silver nanoparticles were grown at the Faculty of Medicine of the Department of Microbiology, Palacký University in Olomouc. To determine cytotoxicity of all the prepared silver containing nanomaterials, human fibroblast (BJ) cell lines were used.

3.2 Instruments and equipment

3.2.1 Spectrometer Specord S600

The Specord S600 spectrometer from Analyst Jena was used to measure spectra. This device is very accurate and fast, thanks to its diode array detector. Its measurement range is in the wavelength range from 190 nm to 1020 nm.

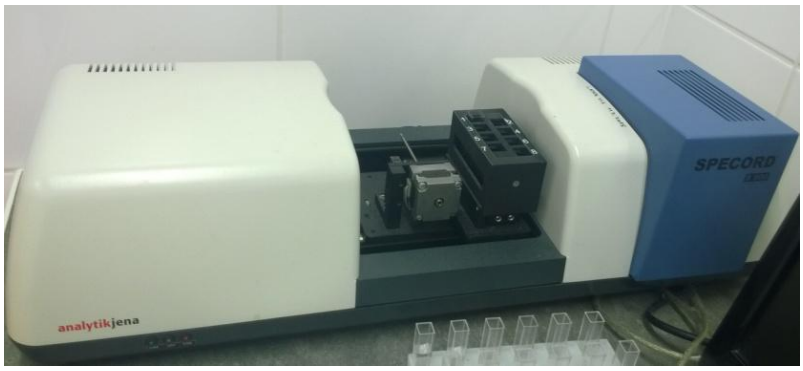

Figure 4. Spectrometer Specord S600

3.2.2 Zetasizer NanoZS

Owing to the combination of high intensity laser and phase light analysis (PALS) technique, Malvern M3-PALS, has high sensitivity and accuracy for measuring zeta potential and the hydrodynamic diameter of colloids.

Figure 5. Zetasizer NanoZS

3.2.3 Nicolet Thermo (FT-IR)

Infrared spectra were measured on the Nicolet instrument from Thermo Scientific with a Zn-Se ATR accessory.

Figure 6. FT-IR instrument Nicolet Thermo Scientific

3.2.4 Transmission electron microscopy (TEM)

Electron microscopy is divided in two basic construction streams. Transmission electron microscopy (TEM) allows electrons to fly through the sample and the final image is proceed on fluorescent screen. This type of electron microscope allows to see structure of illuminated specimens. On the other hand, scanning electron microscope (SEM) is better for imaging surface of specimen due to electrons reacting with the surface of specimen. Electrons are losing energy and are reflected to the detector. So, the secondary electrons create detailed image of specimen surface compared to the TEM.

Both microscopes consist of similar parts such as an electron gun. Electron gun thermionically emitter's electron beam that is modified by electromagnetic coils. The most used electron gunss are Schottky source, tungsten filament or lanthanum hexaborite tip. Electromagnetic coils serve mainly as a condenser lenses.[56]

3.3 Preparation of Graphene/Ag composite

In this thesis two types of graphene derivatives were used (*Cyanographene* and *Graphene acid*) in order to prepare three types of composites with silver: silver nanoparticle, ultra small silver nanoparticles and ionic silver.

3.3.1 Silver nanoparticles-decorated cyanographene (G_CN/AgNPs) and Graphene acid (G_COOH/AgNPs)

Nanocomposites were synthesized by adding the graphene derivatives (5mg) to an 2mL $AgNO_3$ solution followed by 10 min of sonication and 20 min of stirring. Then 2mL ammonia was added to the reaction to form a complex of silver and ammonia. 2mL sodium citrate was added as a stabilizer when $NaBH_4$ was used as a reducing agent. Reduction of silver was initiated by addition of the 0,4 mL $NaBH_4$ solution into the reaction mixture at R.T. and completed after 60 minutes. When maltose was used as a reducing agent, no stabilizer was used, but 0,4 mL sodium hydroxide was added to increase the pH value for the proper reduction of the silver nanoparticles produced in the alkaline medium. Reaction details are available in Table1.

3.3.2 Ionic silver-decorated cyanographene (G_CN/iAg) and graphene acid (G_COOH/iAg)

Ionic silver-decorated cyanographene (G_CN/iAg) and graphene acid (G_COOH/iAg) nanocomposites were synthesized similarly like silver nanoparticle samples **but without the use of sodium borohydride**. In a typical procedure, the graphene derivate was added to the $AgNO_3$ solution followed by 10 min of sonication and 24 h of stirring. Sonication and subsequent reactions took place in the dark to avoiding formation of small silver seeds and consequent of formation big particles. In the case of the ion-silver composite, the purifying was performed by centrifugation at a rate of 15,000 rcf.

3.3.3 Ultra small particles decorated graphene acid (G_COOH/AgUs)

Nanocomposites were synthesized from ionic silver composites, by adding 0,4 mL of $NaBH_4$ as a reducing agent 24hr after purification of ionic silver nanosmposites. All the composites (with nanoparticles/ultra small particles or ionic Ag) were vacuum filtered using cellulose filter (200 nm) and washed three times with 50 ml of distilled water in order to remove silver NPs or silver ions which were not firmly grafted on the graphene flakes. The purified dispersions of the nanocomposites were used for further measurements. Products were filtrated three times (Figure 8), where the light yellow color in the first filtrate (corresponding to unbound Ag nanoparticles), decreases and disappears in the second and third washing, respectively, therefore indicating that all the free particles have been removed.

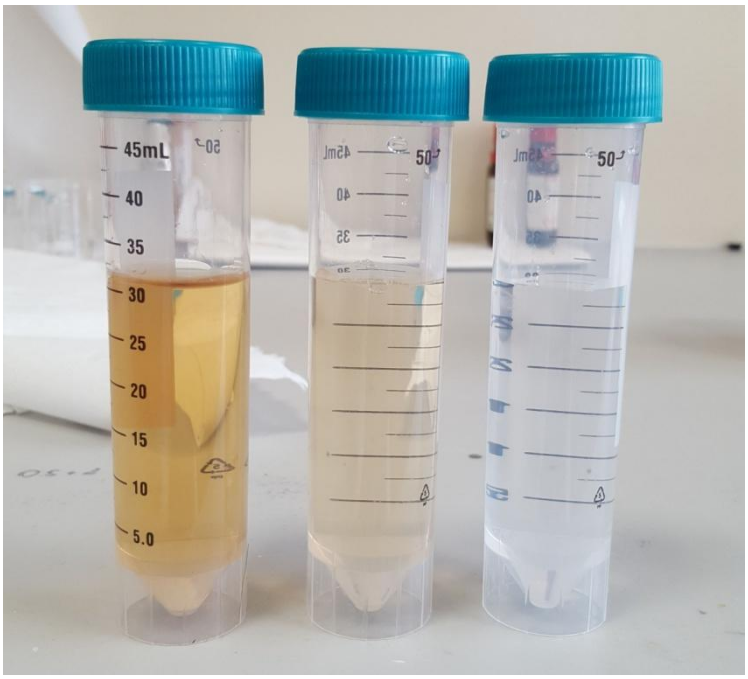

Figure 8. Filtrates containing free silver particles

Table 1. Experimental synthetic details for the preparation of the different graphene/silver nanocomposites.

	Ag@Cyanographene (G_CN/Ag)		**Ag@Graphene Acid (G-COOH/Ag)**			
	npAg/ SBC	**iAg**	**npAg/ SBC**	**iAg**	**iAgSB (ultra small)**	**npAg/ML**
Cyanographene (mg/L)	750		-			
Graphene acid (mg/L)	-		750			
$AgNO_3$ (mol/L)	$2.2x10^{-3}$		$2.2x10^{-3}$			
NH_3 (mol/L)	$3.2x10^{-3}$	-	$3.2x10^{-3}$	-	-	$3.2x10^{-3}$
Citrate (mol/L)	$6.9x10^{-3}$	-	$6.9x10^{-3}$	-	-	-
$NaBH_4$ (mol/L)	$2.2x10^{-3}$	-	$2.2x10^{-3}$	-	$2.2x10^{-3}$	-
Maltose (mol/L)	-	-	-	-	-	$2.06x10^{-2}$
NaOH (mol/L)	-	-	-	-	-	$7.5x10^{-3}$

4.1 Determination of composite and silver concentration in their dispersion and silver concentration in composite

0,5 ml of water dispersion of each composite were dried in vacuum dessicator. Dry matter was weighed to calculate final composite concentration per liter, using a 5 decimal place balance (readability 0.01mg). The content of silver in Ag-graphene nanocomposites was determined using atomic absorption spectrophotometer (AAS) ContrAA 300 (Analytik Jena, Germany) using method of flame atomization. For measurements on AAS 0.25 ml of each nanocomposite water dispersion was filled to 25 ml with nitric acid solution (2 % w/w) and shaken for two hours to quantitatively dissolve silver NPs in composite. Dispersions of graphene with dissolved silver NPs were filtered using syringe filter (Polyethersulfone membrane, 45 μm) before analysis on AAS spectrophotometer. The results are displayed in Table 2.

Table 2. Determination of composite and silver concentration in water dispersion and silver concentration in composite.

	G_CN/Ag		G_COOH/Ag			
	SB	**iAg**	**SB**	**iAg**	**AgUs (ultra small)**	**ML**
Composite/silver concentration in water dispersion (mg/L)	1200,5/330,5	1115/83,25	1680/321,8	1370/84,04	1340/76,82	1770/321,6
Silver amount in composite (mg/g)	275,4	74,7	191,5	61,34	57,33	181,69

NOTE: sb – sodium borohydride, ml – maltose, iAg – ionic silver, Us – ultra small,

4.2 Zeta potential, hydrodynamic size and conductivity

Zeta potential and composite size were measured on the nanoZS instrument from the company Malvern. A sample for zeta/size measurement was prepared by adding 20 μL of the composite to 1.2 mL of water. Conductivity was measured by the conductivity meter by inserting the probe directly into the sample. The results are displayed in Table 3.

Table 3. Determination of Zeta-potential, pH, size and conductivity

	G_CN/Ag		G_COOH/Ag			
	SB	**iAg**	**SB**	**iAg**	**AgUs (ultra small)**	**ML**
zeta potential [mV]	-34,6	-30,4	-30,7	-36,1	-31,1	-29,4
pH	9,04	4,96	9,7	4,87	8,47	9,89
conductivity [us/cm]	20.2	18,4	19,3	8,6	13,3	25,7
d.nm	179,7	350,0	229,5	481,8	373,4	275,3
PDI	0,57	0,46	0,44	0,52	0,45	0,39

NOTE: sb – sodium borohydride, ml – maltose, iAg – ionic silver, Us – ultra small,

4.3 Antimicrobial assay

Antimicrobial activity of the prepared nanocomposites was tested using the standard dilution method which enables to determine the minimum inhibitory concentration (MIC) of the tested sample inhibiting the growth of the tested bacterial strain and yeasts. For the purpose of antimicrobial testing, water suspensions of nanocomposites were used. Testing was carried out in microtiter plates where the tested samples were diluted by the culture medium (Mueller Hinton Broth, Difco, France) in a geometric progression from 2 to 128 times. Culture medium was inoculated with the tested bacteria or yeast at a concentration of 10^5 to 10^6 CFU/mL. After 24h incubation at 37 °C, MIC of nanocomposites as well as MIC values related to the concentration of silver (determined from the amount of silver contained in the respective nanocomposite), i.e., Ag-related MIC values, were determined as the lowest concentrations of the tested substance inhibiting the visible growth of microorganisms. The obtained Ag-related MIC were compared with those of 28 nm sized silver NPs in water dispersion prepared by modified Tollen's process via maltose as reducing substance and with MIC of $AgNO_3$ solution.

For the purpose of antibacterial and antifungal assays of the prepared nanocomposites, a Mueller-Hinton broth (Difco, Becton Dickinson) was employed as a cultivation medium. The following reference strains (labeling according to Czech Collection of Microorganisms, Czech Republic) and isolated strains were used: *Enterococcus faecalis* CCM 4224, *Staphylococcus aureus* CCM 3953, *Escherichia coli* CCM 3954, *Pseudomonas aeruginosa* CCM 3955, *Pseudomonas aeruginosa*, *Staphylococcus epidermidis* 1, *Staphylococcus epidermidis* 2, *Staphylococcus aureus* (MRSA), *Enterococcus faecium* (VRE), *Klebsiella pneumoniae* (ESBL), *Candida albicans. Ag - resistant Eschericha coli, Ag - resistant Staphylococcus aureus.*

4.4 Cytotoxicity assay

The ability of G_CN/Ag and G_COOH/Ag to inhibit cell growth was determined in vitro with BJ cell lines. The cells, cultured in Dulbecco's Modified Eagle's Medium (supplemented with 10% fetal calf serum, 4 mM glutamine, 100 IU/mL penicillin, 100 μg/mL streptomycin) in a humidified CO2 incubator at 37°C, were redistributed into 96-well microtiter plates at the appropriate densities for their respective cell sizes and growth rates. After 12-hour preincubation, the solutions of tested samples were added on the mini rotator (orbital shaking 20 rpm) to avoid sedimentation of the material and subsequent inaccurate measurement of cytotoxicity. Following 24 hours of incubation, the cells were treated for 1 hour with Calcein AM, and live-cell fluorescence was measured at 485

nm/538 nm (ex/em) with the Fluoroskan Ascent microplate fluorometer (Labsystems). LC100 values, the concentrations of silver lethal to 100% of the cells, were determined from the dose-response curves.

5. Results and Discussion

5.1 Synthesis of silver nanoparticles and ionic silver decorated on Cyanographene and Graphene acid sheets

The highly conductive and hydrophilic cyanographene allows exploiting the chemistry of −CN groups toward a broad scale of graphene derivatives with very high functionalization degree. The consequent hydrolysis of cyanographene results in graphene carboxylic acid, showing excellent biocompatibility, conductivity and dispersibility in water.[19] Further, the carboxyl groups enable simple, tailored and widely accessible chemical modifications onto graphene. Thanks to these properties, graphene derivatives were used as a carrier material for the robust immobilization of silver nanoparticles preventing their aggregation compared to free non-immobilized silver NPs in water dispersions. Graphene/Ag composites have been synthesized in this work for the purpose of the stabilization and immobilization of silver NPs on the surface of graphene sheets resulting in high antibacterial efficiency against many bacterial strains.

The size of the graphene sheets used to immobilize silver nanoparticles was approx. 300 nm for both graphene acid and cyanographene. Using the previously described synthetic procedures, silver graphene composites were successfully prepared. Indicative images of the products obtained from TEM measurements are depicted on Figure 9. The size of silver nanoparticles reduced by borohydride coated on the surface of graphene sheets was 20 nm for both graphene derivatives, based on TEM images (Figure 9a-d) and the size of silver nanoparticles reduced by maltose was 30nm (Figure 9e, f). In the case of the ionic Ag composites, where no reducing agent was used, TEM Images verified the absence of nanoparticle formation (Figure 9g,h). In the composites with ultra small silver particles (G_COOH/AgUs) the size is approximately 2-5 nm (Figure 9i-k).

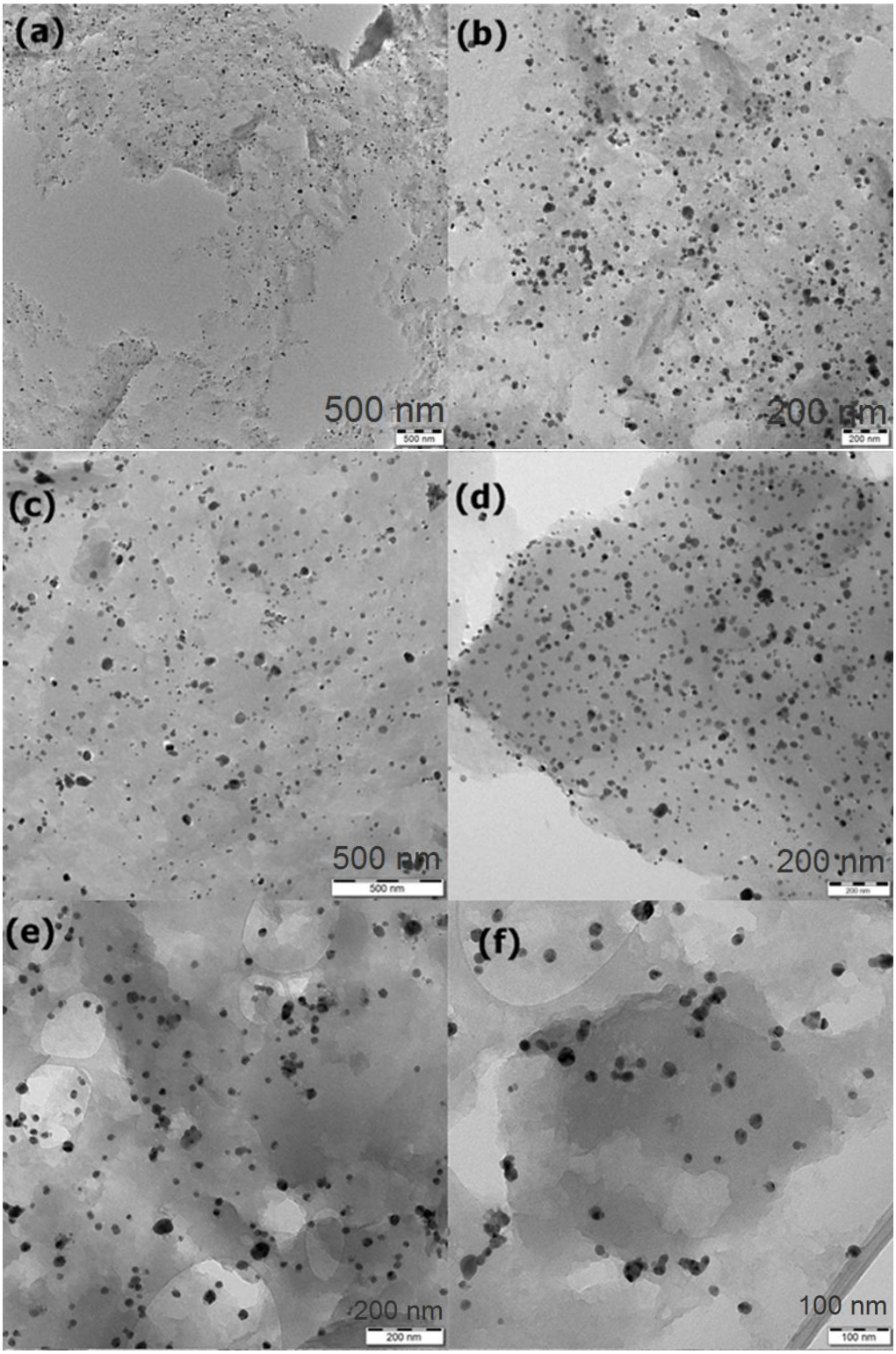
(a)
500 nm
(b)
200 nm
(c)
500 nm
(d)
200 nm
(e)
200 nm
(f)
100 nm

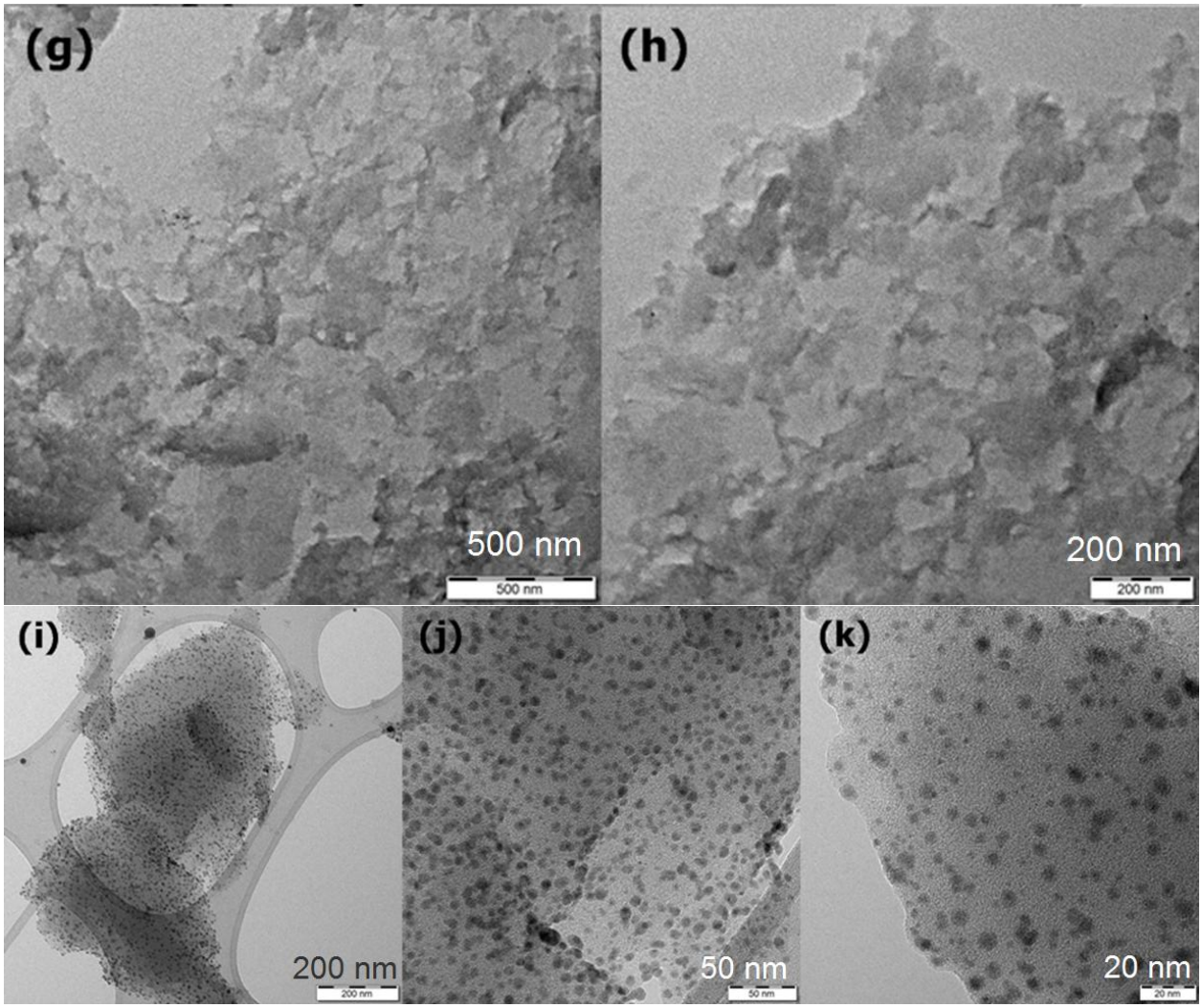

Figure 9. TEM images of silver nanoparticles-decorated cyanographene (a, b) and graphene acid (c, d) both were reduced by sodium borohydride. (e, f) silver nanoparticles- decorated graphene acid, particles were reduced by maltose. (g, h) silver in ionic form and (i, j, k) composite with size of particles 2-5 nm.

UV/VIS spectra of graphene silver nanohybrids (Figure 10) corroborate the findings from TEM. The spectra of ionic Ag composites (blue and black curves in Figure 10a) specifically in the region of about 410 nm confirm the absence of silver particles since there is no band corresponding to the absorbance of silver nanoparticles. In the red curve in the same figure (regarding the composite with ultra-small silver nanoparticles) the respective band emerged as a very broad feature. The band of silver nanoparticles is better evident in the case of the Ag composites with bigger sized Ag nanoparticle (Figure 10b). It is overall observed that the width of the Ag plasmonic band decreases as the size turns bigger. For instance the 30 nm Ag NPs in the G-COOH/AgML hybrid displays the sharper band. The intensity, on the other hand, increases with the size, in

accordance with previous reports in the literature.[15] The band in the region of about 250 nm is attributed to the absorbance from the graphene (The spectra of unmodified G-CN and G-COOH are also displayed on the same figure). Silver nanoparticle size ranging from 30 to 10 nm is optimal regarding high antibacterial activity and low cytotoxicity to mammalian cells[57,58]. In Figure 11, the CN group of the cyano-graphene appears at 2200 cm^{-1}, and at 1720 cm^{-1} the absorption of COOH from G-COOH is also evident. At 1580 cm^{-1} the graphene skeleton is reflected ascribed to the ring stretching vibrations. Importantly, there was no change or damage to the structure of the graphene derivatives when attaching silver to the surface of graphene. Nevertheless the –CN and COOH bands appear altered, suggesting interactions between these groups and silver species.

The method used for composite synthesis is very effective thanks to optimally adjusted graphene and silver concentration ratios and especially due to the excellent chemical properties of graphene derivatives used for the immobilization of silver. Cyanographene and Graphene acid derivatives show unique chemical properties thanks to their highly reactive functional cyano and carboxyl groups. These functional groups enable strong bonding of silver atoms and at the same time control of size and formation of uniformly assembled silver nanoparticles on the surface of graphene sheets. Using this synthetic method with the selected graphene derivatives, uniformly coated composites and with a high content of silver nanoparticles can be prepared resulting in improved antibacterial efficiency at very low composite concentrations, as discussed later.

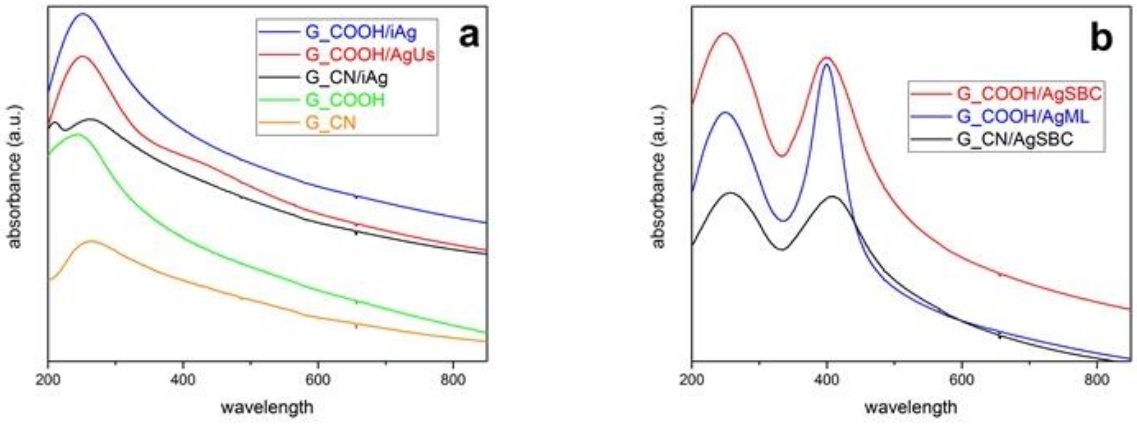

Figure 10. UV-Vis absorption spectra of water dispersions of G_CN/Ag and G_COOH/Ag composites. (a) silver in ionic form (blue and black curves) and ultra small particles (red curve). Green and orange curves are spectra from pure graphene derivatives. (b) absorption of graphene composites with silver nanoparticles reduced by borohydride (red and black curves), and reduced by maltose (blue curve).

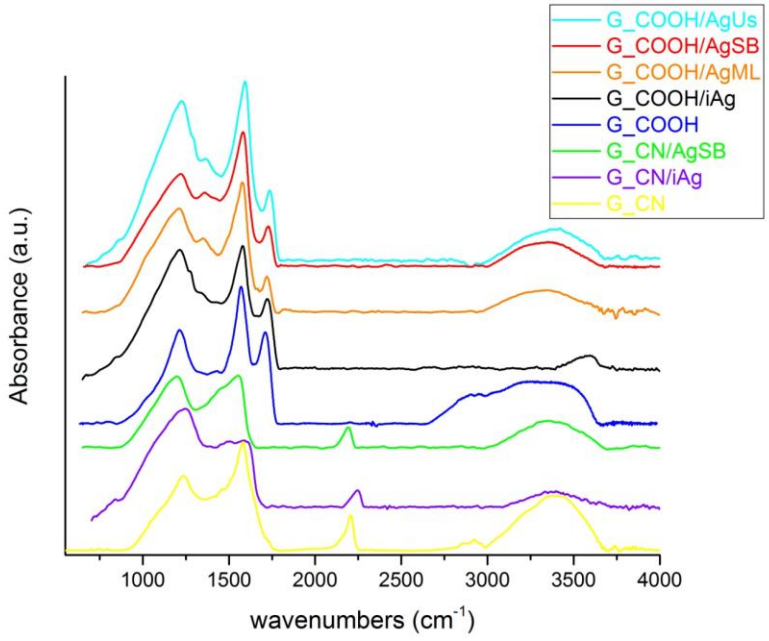

Figure 11. FT-IR spectra of graphene silver nanohybrids and pure graphene derivatives

In addition to the formation of uniformly assembled silver nanoparticles with relatively small size, our synthetic method enables to prepare composites with a very high concentration, due to their high colloidal stability. Determined concentrations for G_CN/Ag and G_COOH/Ag composites in water dispersion were 1200 μg/mL and 1680 μg/mL, respectively (Table 2). Concurrently silver concentrations were also high and were determined to be 330.5 μg/mL (G_CN/Ag) and 321.8 μg/mL (G_COOH/Ag). Silver concentrations in the composites are as follows: 234.4 mg Ag per gram of G_CN/Ag and 191.5 mg Ag per gram of G_COOH/Ag composite, depending of the type of hybrid.

5.1.2 Antimicrobial activity and cytotoxicity of Graphene/Ag nanohybrids

All silver decorated graphene nanocomposites synthesized in this work were tested as antimicrobial agents against drug susceptible and multidrug-resistant bacterial strains including Ag-resistant bacteria. The standard dilution micromethod was applied in this study. Minimum inhibition concentrations (MIC) of the tested silver particles against Gram-positive and Gram-negative bacteria are summarized in Table 4. The used dilution micromethod enables testing of antibacterial activity of samples diluted two times up to 128 times.

Determination of MIC of G_CN/Ag and G_COOH/Ag composites proved their high antimicrobial activity as well, as can be seen in Table 4 summarizing obtained MIC values. MICs of silver in dispersion of composites (G_CN/Ag and G_COOH/Ag) varied from 10.31 μg/mL to 0.61 μg/mL depending on the tested bacteria. The Ag /graphene composites are greatly effective not only for antibiotic-sensitive bacteria, but also have a strong antibacterial effect against resistant strains such MRSA or vanocomycin-resistant *Enterococcus faecium*. Interestingly, when graphene acid was used as a precursor for silver NPs immobilization, the resulted composite G_COOH/Ag showed higher antibacterial activity compared to G_CN/Ag. The reason probably why G_COOH/Ag composite have better antibacterial efficiency is higher dispersibility and stability in water dispersion compared to G_CN/Ag composite. Furthermore, in Table 4 different antibacterial activities of different composites can be seen. The lowest activity is found in the composite where silver was reduced by maltose because of larger particles around 30nm (Figure 8e, f). A composite containing ultra-small particles with a size of 2-5 nm (Figure 9 i-k) exhibits the greatest antibacterial activity, with an ultralow minimal inhibitory concentration from 4.8 μg/mL to 0.6 μg/mL, due to small particles and due to the excellent properties of graphene with high surface and dispersibility in water. Importantly, both of these materials were very effective even against silver-resistant bacteria because of the strong immobilization of silver NPs on the surface of graphene sheets. Determined values of MIC of silver in dispersion of composite (G_CN/Ag and G_COOH/Ag) against Ag-resistant *Escherichia Coli* and Ag-resistant *Staphylococcus aureus* 008 varied from 10.31 μg/mL to 4.80 μg/mL depending of the type of composite and type of Ag-resistant bacteria. Strong immobilization of silver nanoparticles on graphene substrates together with easy dispersibility and stability in water represent a very effective way how to prevent aggregation instability of silver NPs and how to restore their antibacterial activity against silver-resistant bacteria. Simultaneously with antimicrobial evaluation, cytotoxicity of all the synthesized graphene/silver nanocomposites was determined. When compare obtained MIC (Table 4) against tested microorganisms with LC_{100} to BJ lines (Table 5), it is evident that all the tested nanocomposites display a stronger inhibiting effect against microorganisms than to human cells. The lethal concentrations of G_CN/Ag and G_COOH/Ag in this work against the tested human fibroblast were similar and exceeded concentration of 35 μg/mL Ag. Graphene/silver composites exhibit no cytotoxic effects on human fibroblasts at concentrations inhibiting growth of microorganisms which is of a high importance for possible practical application in medicine**.**

Table 4. Minimum inhibitory concentrations of Ag-related (μg/mL) against drug-sensitive, multidrug-resistant and Ag-resistant bacterial strains.

Minimum inhibitory concentrations (μg/mL)								
	$AgNO_3$	**AgNPs**	**G_CN/AgSB**	**G_CN/iAg**	**GA/AgSB**	**GA/iAg**	**GA/AgML**	**GA/AgUs**
concentration of Ag in the dispersion (ug/mL)	**108,00**	**108,00**	**330,60**	**83,25**	**321,80**	**84,04**	**321,60**	**76,82**
Enterococcus faecalis CCM 4224	6,75	13,5	5,16	5,30	5,03	5,25	5,03	3,81
Staphylococcus aureus CCM 3953	3,38	6,75	5,16	2,60	2,51	2,63	2,51	1,91
Escherichia coli CCM 3954	3,38	3,38	5,16	2,60	2,51	1,31	2,51	1,20
Pseudomonas aeruginosa CCM 3955	1,69	6,75	5,16	2,60	2,51	2,63	2,51	0,95
Pseudomonas aeruginosa	1,69	3,38	5,16	2,60	2,51	2,63	2,51	1,91
Staphylococcus epidermidis 1	3,38	3,38	5,16	1,30	2,51	1,31	2,51	2,40
Staphylococcus epidermidis 2	3,38	3,38	5,16	1,30	2,51	1,31	2,51	1,20
Staphylococcus aureus (MRSA)	13,5	6,75	5,16	1,30	5,03	5,25	5,03	3,81
Enterococcus faecium (VRE)	6,75	13,5	10,31	2,60	5,03	5,25	5,03	3,81
Klebsiella pneumoniae (ESBL)	3,38	6,75	10,31	2,60	2,51	5,25	5,03	4,80
Candida albicans	1,69	1,69	3,45	2,60	2,51	0,66	2,51	0,60
Ag - resistant Eschericha coli	6,75	108	10,31	5,20	10,06	5,25	10,05	4,80
Ag - resistant Staphylococcus aureus	6,75	54	10,31	5,20	5,03	5,25	5,03	4,80

NOTE: sb – sodium borohydride, ml – maltose, iAg – ionic silver, Us – ultra small, GA – graphene acid

Table 5. LC_{100} of Ag-related (μg/mL) against human fibroblasts.

LC_{100} (μg/mL)	
G_CN/Ag	G_COOH/Ag
35,5	36,6

The G_COOH/AgUs composite displayed the highest antibacterial activity for all strains of bacteria as shown in Table 4, due to very small particles of silver. In the Figure 12, the antibacterial activity of the G_COOH/AgUs composite is compared to commonly used substances such as silver nitrate and silver nanoparticles colloids. In all cases of bacteria, this material has the lowest minimum inhibition concentrations and almost twenty times more effective against silver-resistant bacteria (Ag – res. *Eschericha coli*), than silver nanoparticle colloids with particle size 28 nm.

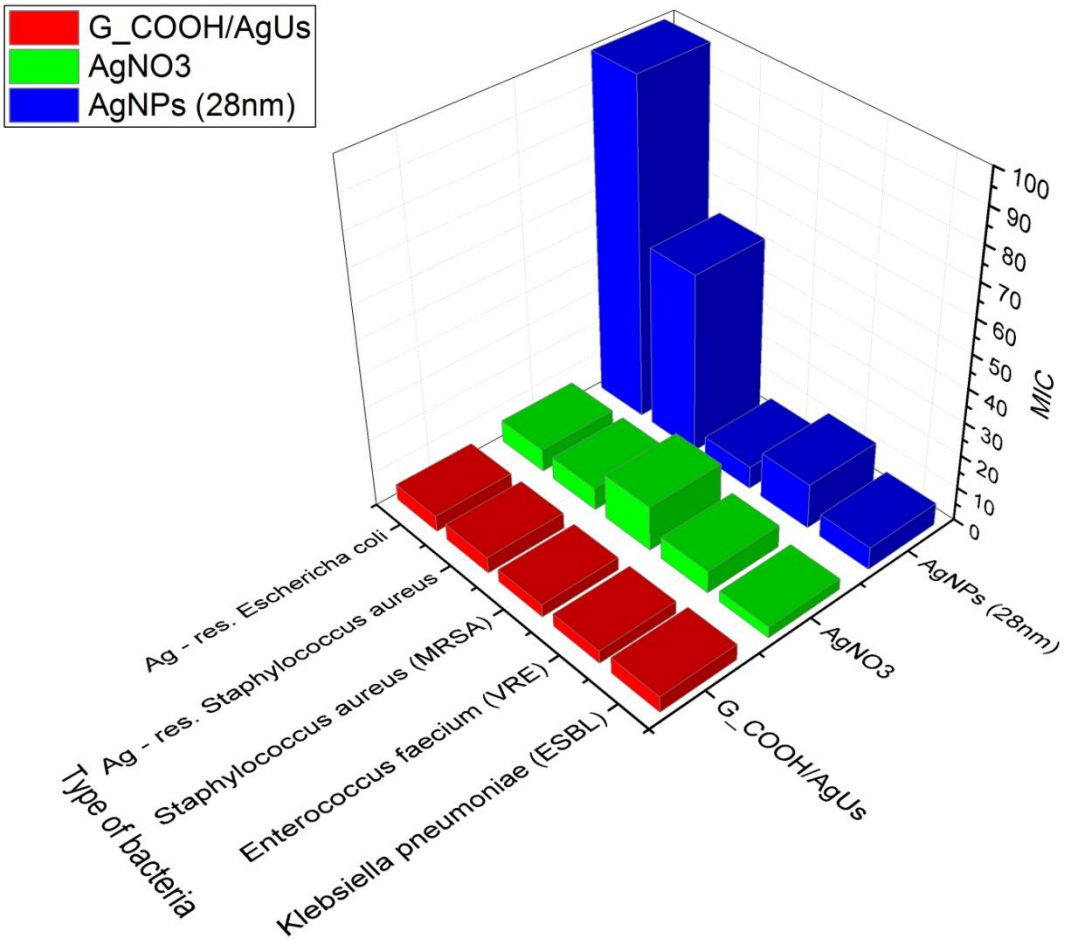

Figure 12. 3D bar graph of MIC comparing the most effective composite (graphene acid with ultra small particles) with silver nanoparticle colloids and ionic silver ($AgNO_3$).

6 Conclusion

In this work, the synthesis of silver-graphene nanocomposite materials is reported. Graphene derivatives covalently functionalized with cyano- and carboxy- groups (cyanographene and graphene-acid, respectively) were used as supports for the growth of nanoparticles of different sizes (c.a. 2 to 30 nm), as well as for immobilization of Ag cations.

The nanocomposites displayed high antimicrobial activity against pathogenic bacteria, including highly resistant and multiresistant bacteria such as methicillin-resistant Staphylococcus aureus (MRSA) or extended-spectrum beta-lactamases (ESBL) producing bacteria. At the same time, synthesized hybrids showed high antibacterial activity even against bacteria which are resistant to silver NPs (such as Escherichia coli and Staphylococcus aureus). The immobilization of the NPs on the graphene supports probably can bypass aggregation of the NPs induced by flagellin production, which is a recently identified mechanism of bacterial resistance to NPs.[45]

It is also interesting to highlight the development of a new way of preparation of very small Ag nanoparticles anchored on graphene with size approx. 2-5 nm. These nanoparticles displayed great stability, without changes in their shape or size for at least one month. This nanohybrid displayed the highest antibacterial activity against all kind of bacteria which were used.

A very important is that both antibacterial activity and cytotoxicity testing were performed under similar conditions and can be compared to each other. Another important report based on the results of testing is that all the tested nanocomposites display a stronger inhibiting effect against microorganisms than to human cells. Due to this fact, that the minimal inhibitory concentration of the composites against bacteria is several times lower than the lethal concentration for human cells, this graphene/Ag nanohybrid can be very suitable for antibacterial applications both in medicine and beyond.

7 Závěr

V této práci je popsána syntéza nanokompozitních materiálů stříbra a grafenu. Kovalentně funkcializované grafenové deriváty se skupinami kyano a karboxyl (kyanografen a kyselina grafenová) byly použity jednak pro růst nanočástic stříbra s různou velikostí (cca 2-30 nm), tak i pro imobilizaci stříbra v iontové formě.

Nanokompozity vykazovaly vysokou antimikrobiální účinnost proti patogenním bakteriím, včetně vysoce rezistentních a multirezistentních bakterií, jako jsou bakterie produkující beta-laktamasy (Staphylococcus aureus) (MRSA) anebo rezistentní vůči meticilinu. Současně syntetizované hybridy vykazovaly vysokou antibakteriální účinnost i proti bakteriím, které jsou rezistentní vůči stříbrným NPs (jako je Escherichia coli a Staphylococcus aureus). Imobilizace nanočástic stříbra na grafenových podkladech může pravděpodobně obejít agregaci AgNPs indukovanou produkcí flagellinu, což je nedávno identifikovaný mechanismus bakteriální rezistence vůči stříbrným nanočásticím.

Je také vhodné zdůraznit vývoj nového způsobu přípravy velmi malých Ag nanočástic ukotvených na grafenu o rozměrech cca. 2-5 nm. Tyto nanočástice vykazovaly velkou stabilitu bez změn ve tvaru nebo velikosti po dobu alespoň jednoho měsíce. Tento nanohybrid vykazoval nejvyšší antibakteriální účinnost proti všem druhům bakterií, které byly použity.

Velmi důležité je, že jak antibakteriální aktivita, tak testování cytotoxicity byly prováděny za velice podobných podmínek a lze je porovnávat. Další důležitou zprávou založenou na výsledcích testování je, že všechny testované nanokompozity vykazují silnější inhibiční účinek proti mikroorganismům než na lidské buňky. Vzhledem k tomu, že minimální inhibiční koncentrace kompozitů proti bakteriím je několikrát nižší než letální koncentrace pro lidské buňky, může být tento grafen / Ag nanohybrid velmi vhodný pro antibakteriální aplikace jak v medicíně, tak i mimo ni.

8 Bibliography

1. Szunerits, S. & Boukherroub, R. Antibacterial activity of graphene-based materials. *J. Mater. Chem. B* **4,** 6892–6912 (2016).
2. O 'neill, J. Ttackling. Drug-resistant infections globally: Final report and recommendations the review on antimicrobial resistance. (2016).
3. L. Kvítek, A. P. *Základy koloidní chemie*. (2007).
4. Sergej S. Vojuckij ; z ruš. přel. Vladimír Karpenko, J. Š. *Kurs koloidní chemie*.
5. Flippen, R. B. Modern methods of polymer characterization. (1991).
6. Baskoro, F. *et al.* Graphene oxide-cation interaction: Inter-layer spacing and zeta potential changes in response to various salt solutions. *J. Memb. Sci.* **554,** 253–263 (2018).
7. Kvítek, L. *et al.* Effect of surfactants and polymers on stability and antibacterial activity of silver nanoparticles (NPs). *J. Phys. Chem. C* **112,** 5825–5834 (2008).
8. L. Kvítek, R. P. Springer, 2005, on-line verze: http://springerlink.com. article no.: s10853-005-0789-2. *J. Mater. Sci.* (2005).
9. Percov, A. V., Pancl, J., Amelina, E. A., Ščukin, E. D. & (Polygrafia). *Koloidní chemie*. (Academia, 1990).
10. Bartovská, L. & Šišková, M. *Fyzikální chemie povrchů a koloidních soustav*. (Vysoká škola chemicko-technologická, 2005).
11. Příručka pro uživatele Zetasizer Nano. (2007).
12. Novák, J. & Vysoká škola chemicko-technologická v Praze. *Fyzikální chemie : bakalářský a magisterský kurz*. (Vydavatelství VŠCHT, 2008).
13. Bosholm, J. D. H. Everett: Basic Principles of Colloid Science. London, Royal Society of Chemistry, 1988, 243 S., 106 Abb., 4 Tab., 120 Lit., broschiert, £ 9,95, ISBN 0–85186–443–0. *Acta Hydrochim. Hydrobiol.* **18,** 110–110 (1990).
14. Soukupová, J., Kvítek, L., Panáček, A., Nevěčná, T. & Zbořil, R. Comprehensive study on surfactant role on silver nanoparticles (NPs) prepared via modified Tollens process. *Mater. Chem. Phys.* **111,** 77–81 (2008).
15. Panacek, A. *et al.* Silver colloid nanoparticles: synthesis, characterization, and their antibacterial activity. *J. Phys. Chem. B* **110,** 16248–16253 (2006).
16. Cosgrove, T. (Terence). *Colloid science : principles, methods and applications*. (Wiley, 2010).
17. Novoselov, K. S. *et al.* Electric field effect in atomically thin carbon films. *Science* **306,** 666–9 (2004).
18. Starodub, E. *et al.* In-plane orientation effects on the electronic structure, stability, and Raman scattering of monolayer graphene on Ir(111). *Phys. Rev. B* **83,** 125428 (2011).
19. Berger, C. *et al.* Electronic Confinement and Coherence in Patterned Epitaxial Graphene. *Science (80-.).* **312,** 1191–1196 (2006).
20. Ruoff, R. Calling all chemists. *Nat. Nanotechnol.* **3,** 10–11 (2008).

21. Chakraborty, S., Guo, W., Hauge, R. H. & Billups, W. E. Reductive Alkylation of Fluorinated Graphite. *Chem. Mater.* **20,** 3134–3136 (2008).

22. Higginbotham, A. L., Lomeda, J. R., Morgan, A. B. & Tour, J. M. Graphite Oxide Flame-Retardant Polymer Nanocomposites. *ACS Appl. Mater. Interfaces* **1,** 2256–2261 (2009).

23. Stankovich, S. *et al.* Stable aqueous dispersions of graphitic nanoplatelets via the reduction of exfoliated graphite oxide in the presence of poly(sodium 4-styrenesulfonate). *J. Mater. Chem.* **16,** 155–158 (2006).

24. Hontoria-Lucas, C., López-Peinado, A. J., López-González, J. d. D., Rojas-Cervantes, M. L. & Martín-Aranda, R. M. Study of oxygen-containing groups in a series of graphite oxides: Physical and chemical characterization. *Carbon N. Y.* **33,** 1585–1592 (1995).

25. Brodie, B. C. On the Atomic Weight of Graphite. *Philos. Trans. R. Soc. London* **149,** 249–259 (1859).

26. Hummers, W. S. & Offeman, R. E. Preparation of Graphitic Oxide.

27. Wissler, M. Graphite and carbon powders for electrochemical applications. *J. Power Sources* **156,** 142–150 (2006).

28. Mkhoyan, K. A. *et al.* Atomic and Electronic Structure of Graphene-Oxide. *Nano Lett.* **9,** 1058–1063 (2009).

29. Eda, G., Fanchini, G. & Chhowalla, M. Large-area ultrathin films of reduced graphene oxide as a transparent and flexible electronic material. *Nat. Nanotechnol.* **3,** 270–274 (2008).

30. Gómez-Navarro, C. *et al.* Atomic Structure of Reduced Graphene Oxide. *Nano Lett.* **10,** 1144–1148 (2010).

31. Marcano, D. C. *et al.* Improved Synthesis of Graphene Oxide. *ACS Nano* **4,** 4806–4814 (2010).

32. Bakandritsos, A. *et al.* Cyanographene and Graphene Acid: Emerging Derivatives Enabling High-Yield and Selective Functionalization of Graphene. *ACS Nano* **11,** 2982–2991 (2017).

33. Akhavan, O. & Ghaderi, E. Toxicity of Graphene and Graphene Oxide Nanowalls Against Bacteria. *ACS Nano* **4,** 5731–5736 (2010).

34. Hu, W. *et al.* Protein Corona-Mediated Mitigation of Cytotoxicity of Graphene Oxide. *ACS Nano* **5,** 3693–3700 (2011).

35. Hu, W. *et al.* Graphene-Based Antibacterial Paper. *ACS Nano* **4,** 4317–4323 (2010).

36. Liu, S. *et al.* Antibacterial Activity of Graphite, Graphite Oxide, Graphene Oxide, and Reduced Graphene Oxide: Membrane and Oxidative Stress. *ACS Nano* **5,** 6971–6980 (2011).

37. Chen, J. *et al.* Graphene oxide exhibits broad-spectrum antimicrobial activity against bacterial phytopathogens and fungal conidia by intertwining and membrane perturbation. *Nanoscale* **6,** 1879–1889 (2014).

38. Pham, V. T. H. *et al.* Graphene Induces Formation of Pores That Kill Spherical and Rod-Shaped Bacteria. *ACS Nano* **9,** 8458–8467 (2015).

39. Kolár, M., Urbánek, K. & Látal, T. Antibiotic selective pressure and development of bacterial resistance. *Int. J. Antimicrob. Agents* **17,** 357–63 (2001).

40. Morones, J. R. *et al.* The bactericidal effect of silver nanoparticles. *Nanotechnology* **16,** 2346–2353 (2005).

41. Darroudi, M. *et al.* Time-dependent effect in green synthesis of silver nanoparticles. *Int. J. Nanomedicine* **6,** 677–81 (2011).

42. Shirtcliffe, N., Nickel, U. & Schneider, S. Reproducible Preparation of Silver Sols with Small Particle Size Using Borohydride Reduction: For Use as Nuclei for Preparation of Larger Particles. *J. Colloid Interface Sci.* **211,** 122–129 (1999).

43. Y. Saito, J. J. Wang, D. N. Batchelder, and & Smith*, D. A. Simple Chemical Method for Forming Silver Surfaces with Controlled Grain Sizes for Surface Plasmon Experiments. (2003). doi:10.1021/LA0301240

44. Wong, K. K. Y. & Liu, X. Silver nanoparticles—the real 'silver bullet' in clinical medicine? *Medchemcomm* **1,** 125 (2010).

45. Panáček, A. *et al.* Bacterial resistance to silver nanoparticles and how to overcome it. *Nat. Nanotechnol.* **13,** 65–71 (2018).

46. Feng, Q. L. *et al.* A mechanistic study of the antibacterial effect of silver ions on Escherichia coli and Staphylococcus aureus. *J. Biomed. Mater. Res.* **52,** 662–8 (2000).

47. Liang, Y., Yang, D. & Cui, J. A graphene oxide/silver nanoparticle composite as a novel agricultural antibacterial agent against Xanthomonas oryzae pv. oryzae for crop disease management. *New J. Chem.* **41,** 13692–13699 (2017).

48. Fathalipour, S. & Mardi, M. Synthesis of silane ligand-modified graphene oxide and antibacterial activity of modified graphene-silver nanocomposite. *Mater. Sci. Eng. C* **79,** 55–65 (2017).

49. Chen, S., Quan, Y., Yu, Y.-L. & Wang, J.-H. Graphene Quantum Dot/Silver Nanoparticle Hybrids with Oxidase Activities for Antibacterial Application. *ACS Biomater. Sci. Eng.* **3,** 313–321 (2017).

50. Zhang, H.-Z. *et al.* Easily separated silver nanoparticle-decorated magnetic graphene oxide: Synthesis and high antibacterial activity. *J. Colloid Interface Sci.* **471,** 94–102 (2016).

51. Marta, B. *et al.* Designing chitosan–silver nanoparticles–graphene oxide nanohybrids with enhanced antibacterial activity against Staphylococcus aureus. *Colloids Surfaces A Physicochem. Eng. Asp.* **487,** 113–120 (2015).

52. Habiba, K. *et al.* Synergistic antibacterial activity of PEGylated silver–graphene quantum dots nanocomposites. *Appl. Mater. Today* **1,** 80–87 (2015).

53. de Faria, A. F. *et al.* Eco-friendly decoration of graphene oxide with biogenic silver nanoparticles: antibacterial and antibiofilm activity. *J. Nanoparticle Res.* **16,** 2110 (2014).

54. Chandraker, K., Nagwanshi, R., Jadhav, S. K., Ghosh, K. K. & Satnami, M. L. Antibacterial properties of amino acid functionalized silver nanoparticles decorated on graphene oxide sheets. *Spectrochim. Acta Part A Mol. Biomol. Spectrosc.* **181,** 47–54 (2017).

55. Bakandritsos, A. *et al.* Cyanographene and Graphene Acid: Emerging Derivatives Enabling High-Yield and Selective Functionalization of Graphene. *ACS Nano* **11,** 2982–2991 (2017).

56. Kubínek, R., Šafářová, K. & Vůjtek, M. Elektronová mikroskopie.

57. Panáček, A. *et al.* Antifungal activity of silver nanoparticles against Candida spp. *Biomaterials* **30,** 6333–6340 (2009).

58. ScienceDirect (Online service), S. *et al. Acta biomaterialia. Acta Biomaterialia* (Elsevier, 2004).